UDK 621.742
Original scientific article/Izvirni znanstveni članek

ISSN 1580-2949
MTAEC9, 57(1)35(2023)

SHRINKAGE BEHAVIOR OF AN ECO-FRIENDLY ENGINEERED CEMENTITIOUS COMPOSITE

KRČENJE OKOLJU PRIJAZNO IZDELANEGA CEMENTNEGA KOMPOZITA

R. Reno Infanto[1*], S. Adish Kumar[2]

[1]Rohini College of Engineering and Technology, Department of Civil Engineering, Palkulam, Tamil Nadu, India
[2]Anna University, Department of Civil Engineering, Regional Center, Tirunelveli, Tamil Nadu, India

Prejem rokopisa – received: 2022-11-17; sprejem za objavo – accepted for publication: 2022-12-09

doi:10.17222/mit.2022.669

The purpose of the present research is to assess the impact of foundry sand (FS) and cement kiln dust (CKD) on the autogenous shrinkage, drying and total shrinkage of engineered cementitious composites (ECCs) over 100 d. Additionally, the pore sizes and their distribution in the developed ECC system were assessed through the BJH adsorption technique. The findings showed that the pore structure was refined continuously over time. This indicates that the CKD-modified ECC mixes demonstrated decreased autogenous shrinkage at the early and later ages of the 100-d period, although the total shrinkage, developed during the later stages, was comparable to the CKD/FS mixes and conventional ECCs. Specimens with 30 % FS and 15 % CKD inclusions showed significantly fewer medium capillary holes and more gel pores. As the pores in a CKD-modified ECC system are smaller than in the traditional ECC, the modified ECC specimens are denser and show a lower loss of water.

Keywords: cement kiln dust, foundry sand, shrinkage, pore structure

Namen raziskave je ocena vpliva livarskega peska (FS; angl.: foundry sand) in prahu iz filtrov peči za žganje cementa (CKD, angl.: Cement Kiln Dust) na avtogeni razvoj, sušenje in celotni skrček izdelanih kompozitov na osnovi cementa (ECC, angl.: engineered cementitious composites) v času njihovega nastajanja (do sto dni). Poleg tega je predstavljena poroznost in njihova porazdelitev v razvitem sistemu ECC s pomočjo dušikove adsorpcijske tehnike BJH (Barett-Joyner-Halenda). Rezultati raziskave so pokazali, da se s časom poroznost strukture neprekinjeno zmanjšuje. To kaže na to, da se pri s CKD nadomeščenih mešanicah ECC zmanjšuje avtogeni skrček tekom celotnega sto dnevnega nastajanja kompozita, tako v zgodnjih kot poznejših fazah, čeprav so vrednosti celotnega skrčka v poznejših stadijih primerljive med mešanicami CKD/FS in ECC. Vzorci s 30 % FS in 15 % nadomestkom CKD kažejo pomembno manjšo količino srednjih kapilarnih por in večgelnih por. Ker so pore v s CKD modificiranem sistemu ECC manjše v primerjavi s tradicionalnimi ECC, so vzorci prvih gostejši in kažejo manjše izgube vode.

Ključne besede: prah iz cementne peči, livarski pesek, skrček, struktura por

1 INTRODUCTION

The past several decades have seen the development of a new class of short-fibre-reinforced cementitious composites known as engineered cementitious composites.[1] Regardless of the loading or deformation, the narrow crack width, which is an inherent attribute of an ECC material, can be automatically maintained within certain ranges. An ECC has a special ability to sustain low material permeability even in the cracked state.[2] Due to the fact that the matrix toughness and fiber-matrix interactions change with an increasing curing age, the ductility of an ECC changes as well.[3] A growing amount of foundry sand (FS) has been identified as a global environmental hazard because to the industrialization's rapid growth. The reutilization rate of WFS increased from 20 % to 30 % as a result of its use as a fine aggregate to substitute natural sand in the making of concrete.[4] Foundry sand waste pozzolanic qualities made it possible to use it in civil construction as a partial replacement for cement, also enhancing mechanical parameters.[5] As much as 35 % more fine aggregate of waste foundry sand can be substituted, and an increase in the strength characteristics is observed.[6] At ages of (7, 28 and 90) d, the concrete containing 60 % of waste foundry sand shows a sharp decline in workability and mechanical strength. However, after 365 d, the strength is within the acceptable range.[7]

The chemical composition and physical qualities of CKD make it suitable for use in concrete applications. CKD as a cement substitute has the potential to revolutionize all the facets of construction by decreasing the enormous volume of cement manufacturing. The CKD inclusion has also started a positive trend in the cement strength and hydration behavior.[8] Using different water-binder ratios, CKD substituted Portland cement in varying amounts ranging from 0 to 25 % to make the concrete mixture.[9] According to the SEM and MIP results, CKD was employed in place of cement to reduce the porosity and densify the concrete microstructure by up to 15 %.[10] Because of its high silica and calcium contents, CKD can act more like cement when improving its hardening properties.

*Corresponding author's e-mail:
renoinfanto.rcet@gmail.com (R. Reno Infanto)

Table 1: Oxide composition of raw materials

Content (kg/m^3)	SiO_2	CaO	MgO	Al_2O_3	Fe_2O_3	SO_3	TiO_2	P_2O_5	MnO	K_2O	Na_2O	LOI
OPC	21.3	63.3	1.65	4.99	4.08	2.7	–	–	–	0.23	0.51	1.29
CKD	15.4	58.9	0.8	3.25	2.53	5.66	–	–	–	5.22	1.05	7.27
FS	95.10	0.19	0.19	1.47	0.49	0.03	0.04	–	–	0.68	0.26	1.32
Fly ash	49.45	3.47	1.3	29.61	10.72	0.27	1.76	0.53	0.17	0.54	0.31	1.45

Table 1 note: OPC – ordinary Portland cement, CKD – cement kiln dust, FS – foundry sand

Understanding the behavior of concrete structures over time and developing appropriate models are crucial for enhancing the strength, safety and durability of concrete structures.[11] Premature cracking is a common problem of many flat concrete constructions. Two factors contribute to the occurrence of shrinkage cracks: the first is a significant early-age shrinkage caused by a high drying surface area; and the second is a significantly constrained shrinkage caused by the surrounding frame or subgrade.[12] Shrinkage fractures drastically impair the longevity of structures by hastening the degeneration of concrete.[13] Shrinkage can cause concrete structures to change shape and volume over time, which can have a big effect on how long they last and how well they work.[14]

After the final setting, two different types of shrinkage can be observed in cement-based materials, namely autogenous and drying shrinkage. The sum of the two shrinkages (autogenous and drying) gives the total shrinkage in a cement system.[15] The autogenous shrinkage generally occurs after the final setting and it is caused by a loss of moisture to the environment, which is accompanied by a change in the volume, self-desiccation and chemical shrinkage.[16] When cement paste is continuously hydrated in an environment with a constant temperature and humidity, shrinkage occurs due to self-desiccation, reducing the macroscopic volume of the concrete.[17] When the w/b content is large, the autogenous shrinkage is always less than 100 μm/m.[18] Even a greater autogenous shrinkage of more than 1000 μm/m occurs in some ultra-high performance concretes. The volume and mineralogical characteristics of the additives also have a considerable impact on the development of shrinkage strains in the cement paste and concrete containing calcium-rich additives.[19] The purpose of this study is to evaluate how CKD and FS can affect the increase in drying and autogenous shrinkage of an ECC system. The main aims of utilizing CKD as a cement replacement are to reduce the cost of production and achieve ecological sustainability by minimizing the disposal cost of CKD. In this investigation, CDK inclusions of up to 22.5 % of the binder (cement + fly ash) weight and up to 45 % of FS were used. The shrinkage behavior of the developed ECC mixes were monitored for 100 d and the distribution of pore sizes of the mixes were evaluated using the BJH N_2 adsorption method.

Despite the fact that there are more and more studies on autogenous shrinkage, the process of concrete shrinkage remains a mystery, and there is no agreement on a measurement standard. Conversely, drying shrinkage, which primarily affects concrete that is close to the surface, is brought on by the water loss to the environment. Pozzolanic reactions can lead to a pore distribution and refinement over time when using SCMs, which can change how much cement paste shrinks.

2 EXPERIMENTAL PART

In this investigation, fly ash, CKD and OPC 53-grade cement were utilized as binders. The cement used in the study confirmed to IS code 12269-1987, which specifies that cement must have a soundness of at least 10 mm or 0.8 % for the Le Chatellier expansion and autoclave expansion, respectively, and a fineness of greater than 225 m^2/kg. CKD was provided by Elasai Enterprises in India, having an average particle size of around 6 μm in a ball mill. Fine silica sand and foundry sand were used as fine aggregate materials. Particle-size distributions of all the ingredients are presented in **Figure 1** and their chemical properties are shown in **Table 1**. A polycarboxylate-based superplasticizer was used as the high-range water-reducing agent. The mixture composition and specimen designations are presented in **Table 2**.

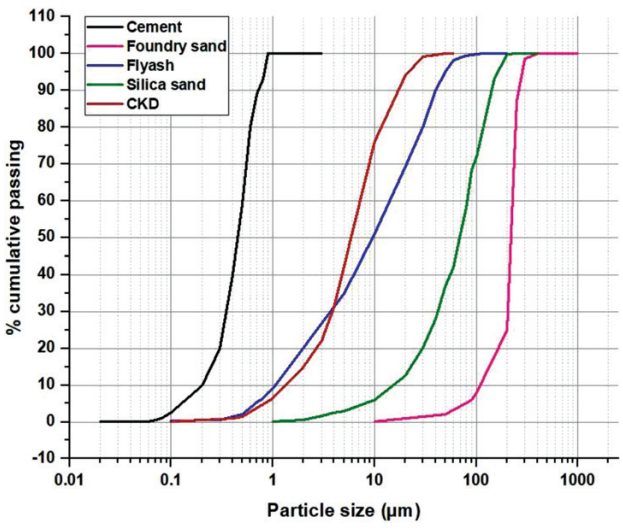

Figure 1: Grain-size-distribution curves for raw materials

2.1 Mix details

To examine the impact of CKD and FS on the shrinkage development of an ECC, ten different ECC mixes, one of which served as the control ECC mix without any replacement, were fabricated. A water/binder ratio of 0.35 was adopted for all the mixes. The ECC mix with OPC53, fly ash and fine silica sand formed the control ECC, while the mixes with OPC53, fly ash, CKD, fine silica sand and FS were designated as modified ECCs (mECCs). The CKD inclusion level ranged from 2.5–22.5 *w*/% of the binder (fly ash + cement) with a 2.5 *w*/% increment, while the FS inclusion ranged from 5–45 *w*/% of fine silica sand with an increment of 5 *w*/%. Different ECC mixes were developed by increasing the substitution levels of CKD with fly ash and FS with silica sand simultaneously until their maximum replacement levels of 22.5 *w*/% and 45 *w*/%, respectively, were achieved. The developed ternary mix combinations are shown in **Table 2**.

Identical volumes of the ECC and total binder content served as the basis for all the mix designs. Within the same ECC mix, the volumetric ratios of the water/binder and binder/fine aggregate were also constant. To get a workable consistency, a superplasticizer of 0.6 % of the binder content (7.55 kg/m^3) was added during the mixing stage. The dosage of the superplasticizer (SP) was chosen as per the previously established study on OPC systems that stated that an SP dosage of more than 0.6 *w*/% of the binder had a strong influence on the expansion of shrinkage.[20] The ECC mixes in the fresh state were mixed, then transferred into various molds and covered appropriately to avoid a loss of moisture from the surface. The casting of ECC mixes took place in an environment with a temperature of (25 ± 2) °C and a relative humidity (RH) of about 50 %. After one day, the hardened ECC mixes were removed from the molds, and various curing and pre-conditioning treatments of the specimens were carried out in accordance with the standard procedures.[21]

Table 2: Mix proportions of ECC mixes

Mix Id	Cement	Fly ash	CKD	Silica sand	FS	Water
	kg/m^3					
CTRL	393.0	865.0	0	457.0	0	311
F5C2.5	382.2	854.2	21.6	434.2	22.9	311
F10C5	371.4	843.4	43.3	411.3	45.7	311
F15C7.5	360.6	832.6	64.9	388.5	68.6	311
F20C10	349.8	821.8	86.5	365.6	91.4	311
F25C12.5	338.9	810.9	108.1	342.8	114.3	311
F30C15	328.1	800.1	129.8	319.9	137.1	311
F35C17.5	317.3	789.3	151.4	297.1	160.0	311
F40C20	306.5	778.5	173.0	274.2	182.8	311
F45C22.5	295.7	767.7	194.6	251.4	205.7	311

2.2 Experimental programs

ECC prisms of (75 × 75 × 280) mm were made in order to monitor the shrinkage over the course of 100 d. The shrinkage values were measured with a digitally controlled gauge meter with a resolution of 1 μm/m. After demolding, autogenously shrunk prisms had their entire surface covered with an aluminium foil, which was waterproof and self-adhesive to avoid a loss of moisture during the experiment. EN 12390-2021 was used as the standard for measuring the shrinkage values and the weight of the specimens after autogenous shrinkage was recorded. The overall shrinkage was established for the unsealed samples that were left in a controlled environment after demolding. After demolding, samples were kept for additional 7 d in a lime-water bath for the initial shrinkage measurement. The total shrinkage was taken by measuring the reference lengths after demolding; the autogenous shrinkage was taken for wrapped specimens; and the drying shrinkage was taken 7 d after the removal of the specimens immersed in the water bath. Then, all the shrinkage samples were stored in a climate-controlled space with a constant temperature of 23 °C at a 50 % relative humidity. The shrinkage of the ECC was then measured at various ages up to the 100th day and the sum of drying shrinkage and autogenous shrinkage was used to determine the overall shrinkage. The nitrogen-adsorption method was used to evaluate the distribution of the pore sizes of the ECCs. The ECC mixes were made, sealed and cured for 28 d before being evaluated. The paste samples were dried for 30 min at 40 °C prior to the experiment, and then they were immersed in isopropyl alcohol for about 30 min to stop the hydration. A ball mill was then used to grind the samples until they could pass through an 850-μm sieve. A degassing temperature of 40 °C was maintained for about 16 h and the nitrogen-adsorption (BJH) method was used to figure out the distribution of the mesopores (2–50 nm).

3 RESULTS AND DISCUSSION

The hydration products such as portlandite and ettringite undergo structural swelling and the autogenous swelling of the CKD-containing ECC at an early age remains a mystery. Therefore, more research is required to determine how CKD and FS affect the early-stage expansion of ECCs.

3.1 Autogenous shrinkage

Figure 2, highlighting the autogenous shrinkage values for one week (7 d), shows the average autogenous shrinkage strain values of the ECC mixtures for 100 d. Negative and positive numbers represent the contraction and swelling of the developed ECCs. In the early days, within 5 d after demolding, all the ECC mixes showed signs of expansion and after one day, the expansion behavior of the CKD-containing ECC mixes was more

striking than that of the control ECC mix with the greatest value. Previous studies indicated an expansion of the cement with additives at an early stage, with medium to high water/binder ratios, which can be related to the growth of several hydration products.[22] The ECC mixes with CKD displayed considerably larger shrinkage strains during autogenous shrinkage for a longer term during 100 d compared to the control ECC. The increased shrinkage stresses in the ECC mixes with CKD ranged from 264–293 μm/m and a significant increase in the autogenous shrinkage with values of more than 50 μm/m after 100 d was observed at a 0.35 w/b ratio. More precisely, from 6th to 50th day, the ECC mixes showed roughly similar autogenous-shrinkage trends at a 15 % CKD inclusion, and after the 100th day, they showed a larger shrinkage strain than the conventional ECC mix with 10 % of CKD. After 10 d, the ECC with 20 % of CKD had the highest shrinkage value of all the ECC mixtures, and after 100 d, it reached about 293 μm/m. Additionally, over the course of the testing period, the autogenous shrinkage of the ECC with 15 % of CKD grew at a slower rate and the values were stabilized after 50 d or so, whereas the ECC with 20 % of CKD stabilized after 90 d. The results obtained were in accordance with the previous findings that showed that autogenous shrinkage increased with an increase in fine aggregates.[23] For up to a year, the value of the developed ECC was measured and it was found that the long-lasting hydration process in the CKD system was responsible for the increased autogenous shrinking. Previous investigations found a decreasing portlandite concentration, which increased after 90 d. This finding points to ongoing microstructural interactions between cement and CKD that cause long-term autogenous shrinkage. Additionally, the pore structure refinement brought about by the inclusion of CKD can be used to explain why the autogenous deformation of the CKD-containing ECC mixes and that of the control CKD mixes differ.

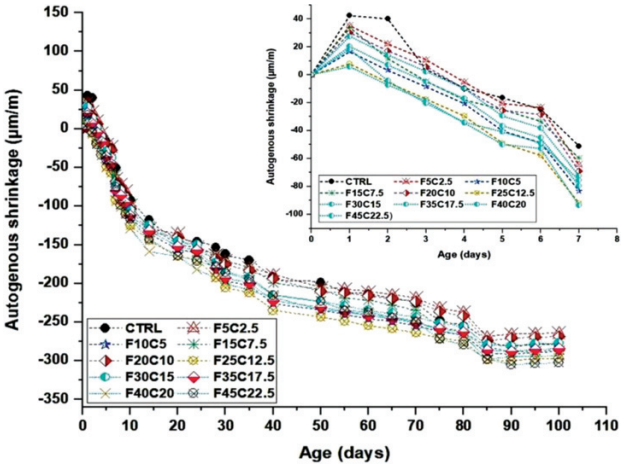

Figure 2: Autogenous shrinkage of ECC mixes (inset covers the first 7 d)

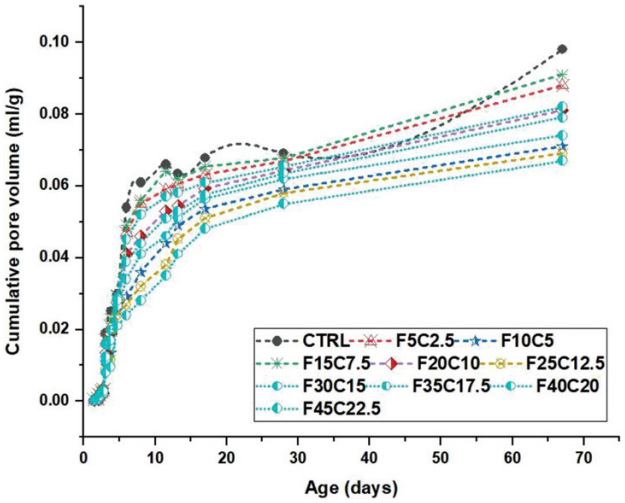

Figure 3: BJH method for the pore-size determination

Figure 3 displays the distribution of voids/pores of the control ECC and CKD-containing ECC mixes after 28 d of curing. Essentially, the pore-size ranges can be divided into four categories, namely micropores, small capillary pores/gel pores, medium capillary pores, and large capillary pores.[24] The pores that influence the shrinkage of an ECC to the greatest extent are the gel and medium-sized pores, speeding up the self-desiccation phenomenon in the ECC when the pore sizes are less than 50 nm. As seen in **Figure 3**, specimens with a 15 % CKD inclusion showed significantly more medium capillary holes and gel pores than the control ECC mix. The capillary theory underlies the process of self-desiccation, the primary factor in the autogenous shrinkage of cementitious materials. Increased autogenous shrinkage in an ECC is caused by the fine pores due to the addition of micro-sized CKD, which eventually lowers the equilibrium of the internal moisture, thereby increasing the capillarity pore pressure.

3.2 Total shrinkage

The progression of the total shrinkage of all the ECC mixes is shown in **Figure 4**. Swelling peaks were not seen in any of the ECC mixtures, suggesting that drying-related shrinkage might have offset or covered the early-age expansion owing to autogenous shrinkage. On the 20th day, a greater shrinkage was observed in the ECC mix with CKD than in the control ECC mix. After that, the ECC mix with CKD outperformed the control ECC mix in its shrinkage values up to the 80th day. On the 100th day, the shrinkage strains of the ECC with CKD and the control ECC were nearly identical, and the rise in the total shrinkage stresses within the cement matrix might be explained with an increase in the fine content in the binder.

As per standards, the total shrinkage of ECC specimens at a constant temperature and RH is regarded as the sum of autogenous and drying shrinkage. However, the

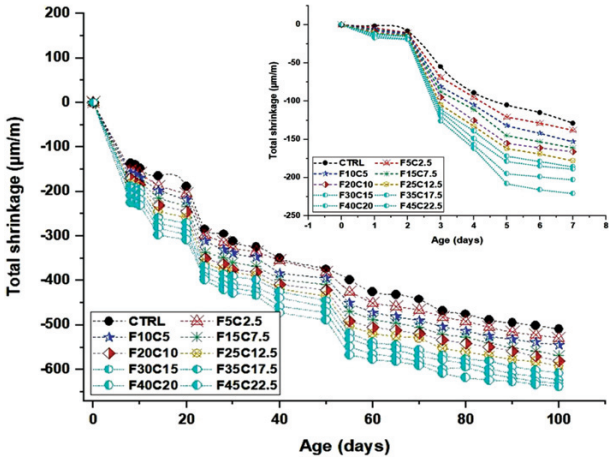

Figure 4: Determination of the total shrinkage after 100 d (inset covers the first 7 d)

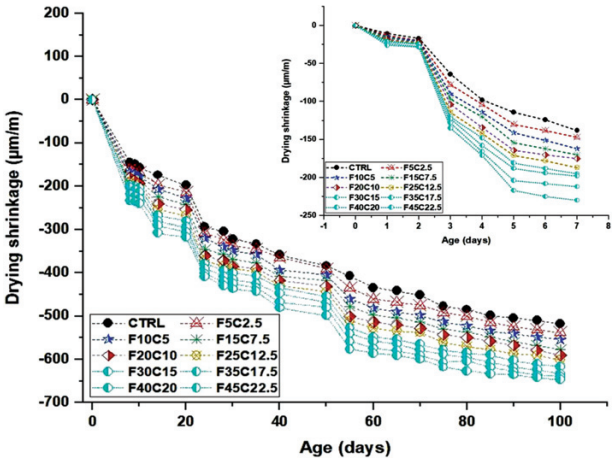

Figure 5: Determination of drying shrinkage over 100 d (inset covers the first 7 d)

drying shrinkage strains of an ECC cannot be directly obtained by deducting autogenous shrinkage from the total shrinkage since the autogenous shrinkage in unsealed shrinkage specimens are lower than the autogenous shrinkage determined under totally sealed conditions. This can be explained with the fact that as water evaporates during drying, less hydration occurs, which slows down autogenous deformation and total shrinkage. The ECC mixes made with CKD and FS appear to undergo this decrease in autogenous shrinkage. Despite this, **Figure 2** clearly shows that the CKD-containing ECC mixes have a larger autogenous shrinkage than the control ECC specimen, although identical total shrinkage values were obtained for both the CKD mixes and control ECC mix at the adopted water content (0.35 w/b ratio). As a result, the CKD-containing ECC mixes produce less drying shrinkage strain than the control ECC. This can also be explained with the finer pore structure of the CKD-containing ECC system compared to the control ECC, creating a denser microstructure and lessening the water loss from the CKD-ECC specimens, also correlating with the results that indicate that the pores in the mECCs are smaller than those in the plain ECC mix.

3.3 Drying shrinkage

Figure 5 depicts the drying shrinkage of the ECC mixes after 7 d of being submerged in lime water. Over the testing period, the developed ECC mixes with up to 15 % of CKD revealed similar shrinkage values up to 30 d, except for the ECC mix, which contained 20 % of CKD, exhibiting larger shrinkage strains than the control ECC. The drying shrinkage values were almost constant after 90 d and the shrinkage development of the specimens was minimal when compared to the thickness of the ECC specimen. After 100 d, the drying and total shrinkage values were almost similar regardless of the binder composition, proving that the water content controls the total and drying shrinkage rather than the binder composition (of plain ECC or mECCs). Like the findings of an earlier study, these results also showed that the inclusion of finer materials in the ECC, at an early age, can cause a large shrinkage but afterward, at a later age, a similar shrinkage value is observed. It should be emphasized that the specimens used in this investigation for drying shrinkage include both types of shrinkage (drying and autogenous) that occurred after one week of testing. The total shrinkage strains of the ECC mixes with CKD are comparable to those of the control ECC mix, especially as the age of the specimens increases.

4 CONCLUSIONS

The study delved more deeply into the assessment of the total shrinkage of an ECC through the measurement of autogenous and drying shrinkage at various ages:

The swelling of the ECC at an early stage was observed due to a CKD inclusion, causing an autogenous expansion. The formation of greater amounts of portlandite and ettringite in the first 7 d caused this swelling mechanism.

Higher shrinkage values were observed between the 7th and 100th d due to a greater refinement of the pores by the finer CKD and FS particles that exhibited smaller mean diameters than the silica sand. In the ECC mixes with CKD, the enhanced shrinkage stresses ranged from 264–293 µm/m, and the autogenous shrinkage significantly increased, reaching values of more than 50 µm/m after 100 d.

The refinement of pores by CKD was confirmed through the BJH absorption techniques, showing that the process was continuous during 100 d.

The proportion of CKD played a major role in determining the shrinkage values at all stages and almost similar shrinkage values were observed at later stages for the CKD mixes and conventional ECC mixes. Thus, the designed ECC mixes cut the building costs the most while keeping the environment in balance and improving the performance of ECCs.

Since an ECC is an unconventional concrete for use in special applications, studies are required to replace fine aggregates with a more economical and viable material. There is no research on the behavior of ECCs when siliceous aggregates are replaced, and no studies of long-term shrinkage are available. There are several potential areas into which this research work can be extended to gain enough knowledge on the use of the developed ECC for structural purposes.

5 REFERENCES

[1] Z. Lin, T. Kanda, V. Li, On Interface Property Characterization and Performance of Fiber Reinforced Cementitious Composites, Journal of Concrete Science and Engineering, 1 (**1999**), 173–184, doi:https://hdl.handle.net/2027.42/84718

[2] D. Zhang, H. Wu, V. C. Li, B. R. Ellis, Autogenous healing of Engineered Cementitious Composites (ECC) based on MgO-fly ash binary system activated by carbonation curing, Construction and Building Materials, 238 (**2020**), 117672, doi:10.1016/j.conbuildmat.2019.117672

[3] X. Huang, R. Ranade, W. Ni, V. C. Li, On the use of recycled tire rubber to develop low E-modulus ECC for durable concrete repairs, Construction and Building Materials, 46 (**2013**), 134–141, doi:10.1016/j.conbuildmat.2013.04.027

[4] N. T. Sithole, N. T. Tsotetsi, T. Mashifana, M. Sillanpää, Alternative cleaner production of sustainable concrete from waste foundry sand and slag, Journal of Cleaner Production, 336 (**2022**), 130399, doi:10.1016/j.jclepro.2022.130399

[5] T. Ramos, A. M. Matos, B. Schmidt, J. Rio, J. Sousa-Coutinho, Granitic quarry sludge waste in mortar: Effect on strength and durability, Construction and Building Materials, 47 (**2013**), 1001–1009, doi:10.1016/j.conbuildmat.2013.05.098

[6] L. Fd. Santos, R. S. Magalhães, S. S. Barreto, G. T. A Santos, F. F. G. de Paiva, A. E. de Souza, S. R. Teixeira, Characterization and reuse of spent foundry sand in the production of concrete for interlocking pavement, Journal of Building Engineering, 36 (**2021**), 102098, doi:10.1016/j.jobe.2020.102098

[7] Y. Aggarwal, R. Siddique, Microstructure and properties of concrete using bottom ash and waste foundry sand as partial replacement of fine aggregates, Construction and Building Materials, 54 (**2014**), 210–223, doi:10.1016/j.conbuildmat.2013.12.051

[8] M. A. El-Mohsen, A. M. Anwar, I. A. Adam, Mechanical Properties of Self-Consolidating Concrete Incorporating Cement Kiln Dust, HBRC Journal, 11 (**2015**), 1–6, doi:10.1016/j.hbrcj.2014.02.007

[9] K. B. Najim, Z. S. Mahmod, A-K. M. Atea, Experimental investigation on using Cement Kiln Dust (CKD) as a cement replacement material in producing modified cement mortar, Construction and Building Materials, 55 (**2014**), 5–12, doi:10.1016/j.conbuildmat.2014.01.015

[10] A. Abdalla, A. Salih, Microstructure and chemical characterizations with soft computing models to evaluate the influence of calcium oxide and silicon dioxide in the fly ash and cement kiln dust on the compressive strength of cement mortar, Resources, Conservation & Recycling Advances, 15 (**2022**), 200090, doi:10.1016/j.rcradv.2022.200090

[11] J. Al-Rezaiqi, A. Alnuaimi, A. W. Hago, Efficiency factors of burnt clay and cement kiln dust and their effects on properties of blended concrete, Applied Clay Science, 157 (**2018**), 51–64, doi:10.1016/j.clay.2018.01.040

[12] F. Sayahi, M. Emborg, H. Hedlund, Y. Ghasemi, Experimental validation of a novel method for estimating the severity of plastic shrinkage cracking in concrete, Construction and Building Materials, 339 (**2022**), 127794, doi:10.1016/j.conbuildmat.2022.127794

[13] Z. Lyu, Y. Guo, Z. Chen, A. Shen, X. Qin, J. Yang, M. Zhao, Z. Wang, Research on shrinkage development and fracture properties of internal curing pavement concrete based on humidity compensation, Construction and Building Materials, 203 (**2019**), 417–431, doi:10.1016/j.conbuildmat.2019.01.115

[14] G. Ke, J. Zhang, Y. Liu, Shrinkage characteristics of calcium sulphoaluminate cement concrete, Construction and Building Materials, 337 (**2022**), 127627, doi:10.1016/j.conbuildmat.2022.127627

[15] M. Sun, P. Visintin, T. Bennett, The effect of specimen size on autogenous and total shrinkage of ultra-high performance concrete (UHPC), Construction and Building Materials, 327 (**2022**), 126952, doi:10.1016/j.conbuildmat.2022.126952

[16] M-Y. Xuan, X-Y, Wang, Autogenous shrinkage reduction and strength improvement of ultra-high-strength concrete using belite-rich Portland cement, Journal of Building Engineering, 59 (**2022**), 105107, doi:10.1016/j.jobe.2022.105107

[17] L. Tian, M. Jiao, H. Fu, P. Wang, H. Zhao, W. Zuo, Effect of magnesia expansion agent with different activity on mechanical property, autogenous shrinkage and durability of concrete, Construction and Building Materials, 335 (**2022**), 127506, doi:10.1016/j.conbuildmat.2022.127506

[18] M. Maslehuddin, O. S. B. Al-Amoudi, M. K. Rahman, M. R. Ali, M. S. Barry, Properties of cement kiln dust concrete, Construction and Building Materials, 23 (**2009**), 2357–2361, doi:10.1016/j.conbuildmat.2008.11.002

[19] Z. Lv, C. Liu, C. Zhu, G. Bai, H. Qi, Experimental Study on a Prediction Model of the Shrinkage and Creep of Recycled Aggregate Concrete, Applied Sciences, 9 (**2019**), 4322, doi:10.3390/app9204322

[20] F. Collins, J. Sanjayan, Effect of pore size distribution on drying shrinking of alkali-activated slag concrete, Cement and Concrete Research, 30 (**2000**), 1401–1406, doi:10.1016/S0008-8846(00)00327-6

[21] Z. Wang, P. Sun, J. Zuo, C. Liu, Y. Han, Z. Zhang, Long-term properties and microstructure change of engineered cementitious composites subjected to high sulfate coal mine water in drying-wetting cycles, Materials & Design, 203 (**2021**), 109610, doi:10.1016/j.matdes.2021.109610

[22] Y. Han, Y. Qin, Y. Wang, X. Zhang, The effect of different ages and water-binder ratios on the mechanical properties of circulating fluidized bed combustion desulfurization slag cement-soil, Case Studies in Construction Materials, 17 (**2022**), e01660, doi:10.1016/j.cscm.2022.e01660

[23] H. Zhang, Y-Y. Wang, D. E. Lehman, Y. Geng, Autogenous-shrinkage model for concrete with coarse and fine recycled aggregate, Cement and Concrete Composites, 111 (**2020**), 103600, doi:10.1016/j.cemconcomp.2020.103600

[24] Z-L. Jiang, Y-J. Pan, J-F. Lu, Y-C. Wang, Pore structure characterization of cement paste by different experimental methods and its influence on permeability evaluation, Cement and Concrete Research, 159 (**2022**), 106892, doi:10.1016/j.cemconres.2022.106892